

Probing non-Abelian statistics with Majorana fermion interferometry in spin-orbit-coupled semiconductors

Jay D. Sau¹, Sumanta Tewari², and S. Das Sarma¹

¹*Condensed Matter Theory Center and Joint Quantum Institute, Department of Physics, University of Maryland, College Park, Maryland 20742-4111, USA*

²*Department of Physics and Astronomy, Clemson University, Clemson, SC 29634*

The list of quantum mechanical systems with non-Abelian statistics has recently been expanded by including generic spin-orbit-coupled semiconductors (*e.g.*, InAs) in proximity to a *s*-wave superconductor. Demonstration of the anyonic statistics using Majorana fermion interferometry in this system is a necessary first step towards topological quantum computation (TQC). However, since all isolated chiral edges that can be created in the semiconductor are charge neutral, it is not clear if electrically controlled interferometry is possible in this system. Here we show that when two isolated chiral Majorana edges are brought into close contact, the resultant interface supports charge current, enabling electrically controlled Majorana fermion interferometry in the semiconductor structure. Such interferometry experiments on the semiconductor are analogous to similar interferometry experiments on the $\nu = 5/2$ fractional quantum Hall systems and on the surface of a 3D strong topological insulator, illustrating the usefulness of the 2D semiconductor heterostructure as a suitable TQC platform. In particular, we proposed Majorana interferometers may be the most direct method for establishing non-Abelian braiding statistics in topological superconductors.

PACS numbers: 03.67.Lx, 71.10.Pm, 74.45.+c

I. INTRODUCTION

Topological many body systems, characterized by exchanges of the particles unitarily rotating the wave function in the degenerate ground state subspace (non-Abelian statistics), are called non-Abelian quantum systems.^{1,2} Such systems have been proposed as a fault-tolerant platform for topological quantum computation (TQC).^{2,3} Some key, albeit exotic, condensed matter systems, such as the Pfaffian states in fractional quantum Hall (FQH) systems^{3,4} and chiral *p*-wave superconductors/superfluids,⁵⁻⁷ as well as the surface state of a 3D strong topological insulator (TI),⁸ have been identified as non-Abelian systems. Recently, this list has been expanded by showing that even a regular semiconducting thin film (*e.g.*, InAs), proximate to an ordinary *s*-wave superconductor and a magnetic insulator, can support non-Abelian excitations.⁹⁻¹¹ Since neither special materials nor exotic physics are needed to produce the non-Abelian excitations, this structure is potentially one of the simplest to probe non-Abelian quantum matter and therefore has attracted considerable attention in the recent literature.¹²⁻²⁶

The non-Abelian excitations in the semiconductor in this proposal, are the zero-energy Majorana fermions, defined by the self-hermitian operators $\gamma_0; \gamma_0^\dagger = \gamma_0$, localized at vortices or the sample edges induced by the superconducting proximity effect.⁹ Even though the non-Abelian excitations in the $\nu = 5/2$ FQH system are charged, the Majorana excitations in the semiconductor are charge-neutral. The charge neutrality of the Majorana excitations makes them unresponsive to an applied electric field and therefore difficult to detect experimentally. On the other hand, electrically controlled edge state interferometry of the Majorana excitations^{3,27,28} is a key experiment both to probe their exotic statistics as well as to implement TQC.²⁹⁻³¹ Recently it has been shown that on the surface of 3D TI (in which the Majorana excitations are also charge-neutral) an interface between two domains with op-

posite directions of magnetization (but no superconductivity) supports gapless *charged* Dirac fermionic modes.^{32,33} These charged modes can break up into two neutral Majorana edge modes in the presence of superconductivity. Since the charged fermion current can be controlled by external electric potentials, this provides a way to electrically control the neutral current of the edge state Majorana fermions in a TI, and thus to detect them.

For a semiconductor, however, the above method does not work because there is no well-defined edge mode at the boundary between two domains with opposite directions of magnetization. This is because, unlike the TI surface, the system remains gapless even with non-zero magnetization in the absence of superconductivity.⁹ In the presence of superconductivity, however, all isolated chiral edge modes (*e.g.*, edges 1 and 2 in Fig. 1) that can be created in this system are Majorana modes, hence charge-neutral. Very recently a set of proposals^{34,35} attempt to avoid this problem by using the transport of Majorana fermions in vortex cores of superconductors to create measurable interferometry of vortices in superconductors. The original proposals³⁴ for such interferometry suffer from the possibly large vortex mass in superconducting systems making the observation of quantum interference in such proposals unlikely. The more recent proposals³⁵ using Josephson vortices instead of Abrikosov vortices can possibly overcome the problem of a large vortex mass but might still face the problem of a very small minigap. Therefore, electrically controlled edge state interferometry of Majorana excitations remains a crucially important experiment to probe the non-Abelian statistics of Majorana fermions and implement TQC on 2D spin-orbit coupled semiconductor systems. This is the problem we tackle in this work.

In this paper, we start with the existence of chiral Majorana edge modes and Majorana fermions shown in Refs.[9-11] and propose an interferometry experiment to demonstrate the non-Abelian character of these charge neutral Majorana fermions.

To this end we first show that chiral Majorana modes located at the isolated edges in the semiconductor (edges 1 and 2 in Fig. 1 with the separation W large) are indeed charge-neutral. However, when the separation W is on the order of the coherence length ξ or smaller, the wave functions localized at the edges overlap and the resulting mode acquires charge. In the limit of zero separation between the edges, it is an interface separating regions with opposite directions of magnetization. We show by explicit calculations that even though such an interface can be thought of as created by superposing two originally charge-neutral Majorana edge modes, it carries a chiral quasiparticle charge current which can be controlled by external bias voltages. The reason such a charge current can arise although the Majorana modes themselves are neutral is, of course, the presence of superconductivity in some sense “violates” the naive charge conservation because of the spontaneous breaking of the $U(1)$ symmetry and the existence of phase coherent Cooper pairs. Recently, similar charged quasiparticle modes have been argued to exist at the domain walls of chiral p -wave superconductors.²⁴ We give two specific interferometer designs suitable for testing non-Abelian statistics of quasiparticles and implementation of TQC.

In Sec. II we describe the basic BdG Hamiltonian for treating the topological superconducting properties of the generic semiconductor-superconductor sandwich structure proposed in Sau et. al.⁹, discussing the condition for the emergence of the non-Abelian Majorana mode. In Sec. III we discuss the magnetic domain wall where the chiral Majorana modes fuse to produce chiral Dirac fermion modes. In Sec. IV we analytically study the charge conductance of the chiral Dirac modes in the wide domain wall limit in which case it is possible to think of the domain wall as composed of a pair of weakly overlapping chiral Majorana modes. We check numerically in Sec. V, that the qualitative features of the wide domain wall limit survive in the narrow domain wall limit, finally describing our proposed interferometer in Sec. VI. We conclude in Sec. VII summarizing our results and discussing some open questions.

II. BDG HAMILTONIAN FOR SANDWICH STRUCTURES

We consider the BdG Hamiltonian for a semiconductor (Sm) in which an s -wave superconducting pair potential Δ and a Zeeman splitting V_Z are induced by proximity effect from a superconducting layer (SC) and a ferromagnetic insulator layer (F)(Fig. 1). This has been shown to be possible experimentally^{36,37} and theoretically.^{11,38} Below, we review the excitation spectrum and derive an effective Hamiltonian of a semiconductor thin film sandwiched between a layer of SC and F. The SC - Sm - F heterostructure, is described by a model defined by the Hamiltonian

$$H_{\text{tot}} = H_{\text{Sm}} + H_{\text{SC}} + H_{\text{F}} + H_{\tilde{t}_{\text{SC}}} + H_{\tilde{t}_{\text{F}}} \quad (1)$$

where H_{Sm} , H_{SC} and H_{F} are the Hamiltonians describing the Sm, SC and F layers respectively. $H_{\tilde{t}_{\text{SC}}}$ and $H_{\tilde{t}_{\text{F}}}$ represent the tunneling Hamiltonians at the Sm-SC and Sm-F interface respectively.

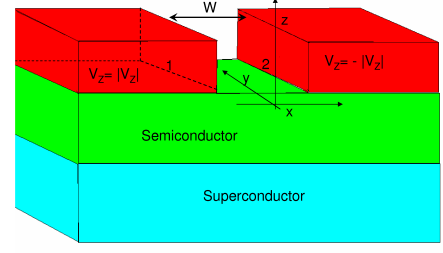


FIG. 1: Structure of an interface along y . Magnetic insulators shown as (red) top layer induce opposite Zeeman splitting in the semiconductor. Edges 1 and 2, each separating regions of non-Abelian and Abelian s -wave superconductors, are separated by interface width W . Such edges, when isolated ($W \gg \xi$, with ξ the coherence length), carry charge-neutral chiral Majorana modes.

The low-energy Hamiltonian for the Rashba SO-coupled Sm layer, H_0 , is given by

$$H_{\text{Sm}}(\mathbf{k}) = \sum_{\mathbf{k}} \psi_{\text{Sm}}^\dagger \left[\frac{k^2}{2m^*} - \mu + \alpha(\boldsymbol{\sigma} \times \mathbf{k}) \cdot \hat{\mathbf{z}} \right] \psi_{\text{Sm}} \quad (2)$$

where m^* is an effective mass. The ferromagnetic insulator F is described by the Hamiltonian

$$H_{\text{F}} = \sum_{\mathbf{k}} \psi_{\text{F}}^\dagger (\epsilon_{\mathbf{k}} - \mu_{\text{F}} + V_{\text{F}} \sigma_z) \psi_{\text{F}} \quad (3)$$

with a mean-field Zeeman order parameter V_{F} and a chemical potential μ_{F} in the Zeeman spin-split gap of the ferromagnetic insulator. Similarly, the s -wave superconductor can be described by a mean-field BCS Hamiltonian

$$H_{\text{SC}} = \sum_{\mathbf{k}} \psi_{\text{SC}}^\dagger (\epsilon_{\mathbf{k}} - E_{\text{F}}) \psi_{\text{SC}} + \Delta_{\text{SC}} \psi_{\text{SC}}^\dagger \psi_{\text{SC}}^\dagger. \quad (4)$$

Here ψ_{SC}^\dagger , ψ_{Sm}^\dagger and ψ_{F}^\dagger are the relevant electron spinor creation operators. In the absence of tunneling between the layers, Sm is normal with no superconductivity. The tunneling term

$$H_{\tilde{t}_{\text{SC}}} = \tilde{t}_{\text{SC}} \psi_{\text{SC}}^\dagger \psi_{\text{Sm}} + h.c \quad (5)$$

which transfers electrons between the Sm-SC layers leads to a finite value for the superconducting order parameter $\langle \psi_{\sigma}(r) \psi_{\sigma'}(r') \rangle$ on the Sm surface by the proximity effect.³⁹ Similarly, the tunneling term

$$H_{\tilde{t}_{\text{F}}} = \tilde{t}_{\text{F}} \psi_{\text{F}}^\dagger \psi_{\text{Sm}} + h.c \quad (6)$$

leads to a proximity-induced ferromagnetic order parameter in the Sm. (In some situations, the magnetic insulator can be replaced by an external magnetic field – the main necessary ingredient is an effective spin splitting in the Sm layer without any magnetic field induced magneto-orbital effects.)

We start by considering the ferromagnetic proximity effect induced in the Sm layer from the F-Sm interface when the states of the lowest semiconductor band with wave vectors

near $\mathbf{k} = 0$ have energies inside the insulating gap of the ferromagnetic insulator F. The insulating degrees of freedom of the ferromagnetic insulator, F , can be integrated out and replaced by an interface self-energy. When projected onto the low-energy subspace, this contribution becomes

$$\Sigma_{\sigma\sigma'}^{(F)}(\mathbf{k}, \omega) = -|\tilde{t}_F|^2 |\psi_{\mathbf{k}}(z_0)|^2 G_{\sigma\sigma'}^{(F)}(\mathbf{k}, \omega; z_0), \quad (7)$$

where \tilde{t}_F is proportional to the transparency of the F-Sm interface, $G_{\sigma\sigma'}^{(F)}(\mathbf{k}, \omega; z_0)$ is the Green function of the ferromagnetic insulator (F) and $|\psi_{\mathbf{k}}(z_0)|^2$ the amplitude of the semiconductor wave function, both at the interface. Note that the imaginary part of the Green function vanishes for values of ω within the insulating gap. Also, because the energies of interest are much smaller than the insulator bandwidth, $\omega \ll \Lambda_\sigma$, we can neglect the frequency dependence in Eq. (7). From Eq. (7) one immediately notices that, neglecting such dynamical effects, i.e., setting $\omega = 0$, the proximity effect self-energy, is equivalent to an effective Zeeman splitting

$$V_Z = \frac{\Sigma_{\uparrow\uparrow}(\mathbf{k} \sim 0, \omega = 0) - \Sigma_{\downarrow\downarrow}(\mathbf{k} \sim 0, \omega = 0)}{2} \quad (8)$$

which creates a gap in the n th semiconductor band near $\mathbf{k} = 0$ that is proportional to the amplitude of the wave function at the interface times the square of the interface transparency.

Thus the dispersion of the low-energy bands in the Sm layer can be obtained by adding the Zeeman splitting (Eq. 8) to the effective theory described by Eq. (2) to obtain a low-frequency and long-wavelength (i.e. $\omega \sim 0$ and $\mathbf{k} \sim 0$) effective Hamiltonian

$$H_{Sm}(\mathbf{k}) = \frac{k^2}{2m^*} - \mu + \alpha(\boldsymbol{\sigma} \times \mathbf{k}) \cdot \hat{\mathbf{z}} + V_Z \sigma_z, \quad (9)$$

with an effective Zeeman splitting V_Z which is determined by the microscopic tunneling parameters at the F-Sm interface and can be tuned by: a) modifying the semiconductor film thickness, b) applying a bias voltage, and c) changing the semiconductor - MI coupling.¹¹ Explicit calculations for various sets of parameters show that this low-energy theory represents an excellent approximation for all \mathbf{k} values of interest.¹¹

Next, we turn our attention to the effects induced by the proximity of an s-wave superconductor on the Sm-F heterostructure. We consider a semiconductor thin film and create a new interface at the free surface of the semiconductor by coupling it to a SC with an s-wave gap Δ . Below we argue that, turning on coupling to the SC opens up a small gap near the fermi surface of the electron-doped semiconductor described by the Hamiltonian in Eq. 9.¹¹

In order to understand this behavior, it is useful to develop an effective low-energy theory for the SC proximity effect that is analogous to the one discussed for the magnetic proximity effect. Thus the effect of the superconductor can be described by an effective self-energy^{38,40}

$$\Sigma_{\sigma\tau; \sigma'\tau'}^{(SC)}(\mathbf{k}, \omega) = -|\tilde{t}_{SC}|^2 |\psi_{\mathbf{k}}(z_0)|^2 G_{\sigma\tau; \sigma'\tau'}^{(SC)}(\mathbf{k}, \omega; z_0), \quad (10)$$

Since the superconducting Hamiltonian H_{SC} is non-number conserving, the Green-function $G^{(SC)}$ contains both

normal and anomalous components that must be described in the Nambu-spinor notation. Therefore, in addition to having spin-indices $\sigma\sigma'$, the Green-function G^{SC} also has Nambu indices τ and τ' , which take values ± 1 similar to their spin counterparts σ and σ' . Introducing the Pauli matrices $\sigma_{x,y,z}$ in the spin components σ, σ' and the Nambu matrices $\tau_{x,y,z}$ in the Nambu indices τ, τ' allows us to write the Green-function for the superconductor as

$$G^{(SC)-1}(\mathbf{k}; \omega) = (\epsilon_k - E_F)\tau_z + \Delta\tau_x - \omega. \quad (11)$$

Substituting the Green-function into Eq. 10 and assuming a slowly varying density of states $\rho_{SC}(E_F)$ at the fermi-level E_F in the superconductor allows us to simplify the self-energy as

$$\Sigma^{(SC)}(\mathbf{k}, \omega) \approx -\frac{-\omega + \Delta\tau_x}{\sqrt{\Delta^2 - \omega^2}}, \quad (12)$$

for the energy levels of interest satisfying $\omega < \Delta$, where $\lambda = |\tilde{t}_{SC}|^2 |\psi_{\mathbf{k}}(z_0)|^2 \rho_{SC}(E_F)$.^{11,38,40}

The self-energy $\Sigma^{(SC)}$ induced in the Sm layer by integrating out the superconductor has an anomalous part (i.e. proportional to τ_x) and therefore induces a non-vanishing superconducting order parameter $\langle \psi_{Sm}^\dagger \psi_{Sm}^\dagger \rangle$ in the Sm despite the fact that the microscopic pairing potential $\Delta_{Sm}(\mathbf{r}) = 0$ in the original Hamiltonian in Eqn. 1. The microscopic pairing potential $\Delta_{Sm}(\mathbf{r}) = 0$ vanishes in the semiconductor since we assume no significant attractive pairing interaction in the semiconductor layer. Our assumption of a vanishing $\Delta_{Sm}(\mathbf{r})$ is also consistent with the de Gennes boundary conditions at the Sm-SC interface which requires $\Delta(\mathbf{r})/N(\mathbf{r})V(\mathbf{r})$ to be continuous across the Sm-SC interface³⁹. Here $\Delta(\mathbf{r})$, $V(\mathbf{r})$, $N(\mathbf{r})$ stand for the microscopic pairing potential, pairing interaction and density of states at the fermi level on both sides of the interface. Since Δ_{Sm} and V_{Sm} are both zero on the Sm side of the interface, the ratio can be finite which allows $\frac{\Delta_{Sm}}{V_{Sm}N_{Sm}} = \frac{\Delta_{SC}}{V_{SC}N_{SC}}$.

Following the arguments in Ref. 40, to compute the Green function in the Sm layer, one can start by integrating out the electronic degrees of freedom in the layers F and SC and replacing them with the effective self-energies in Eq. 7 and Eq. 10 respectively. The Green function for $\omega \ll \Delta$ can then be obtained as the inverse of an effective Hamiltonian for the low-energy excitations in the Sm which is obtained by adding the respective self-energies from the F and SC layers to Eq. 2 and can be written as,

$$H_{BdG} = -(\mu + \nabla^2)\tau_z - i\alpha(\boldsymbol{\sigma} \times \nabla) \cdot \hat{\mathbf{z}}\tau_z + \Delta\tau_x + V_Z(x)\sigma_z, \quad (13)$$

where μ indicates the chemical potential in the Sm layer and $\nabla = (\partial_x, \partial_y)$. The effective pairing potential Δ and Zeeman potential V_Z induced in the Sm layer is found to be proportional to Δ_{SC} and V_F respectively, up to a renormalization that is dependent on the tunneling strengths \tilde{t}_{SC} and \tilde{t}_F .¹¹

The Hamiltonian in Eq. 13 is the effective Hamiltonian of the F-Sm-SC sandwich structure which has recently been shown to support a topologically superconducting phase in the appropriate parameter regime.⁹ More specifically, it was

shown that when the parameters of the system are tuned so that

$$V_Z^2 > \Delta^2 + \mu^2 \quad (14)$$

the quasi-two-dimensional system would support zero-energy Majorana fermions in vortices and chiral propagating Majorana modes around the edges of the system. The chirality of the edge mode would be determined by the sign of the Rashba spin-orbit coupling α and the Zeeman splitting V_Z , the combination of which breaks the inversion and time-reversal symmetries of the system. (The explicit breaking of time-reversal invariance due to the presence of the V_Z term qualitatively distinguishes the topological superconductivity in the Sc-Sm-F sandwich structure⁹ from that in the SC-TI heterostructure³² which preserves time-reversal invariance.)

Finally, we would like to comment that the qualitative features of the results derived in this section for the lowest semiconductor band carry over to the multi-band case¹¹ and the topological properties remain identical as well as long as an odd number of bands are occupied^{22,23,41}.

III. CHIRAL CURRENTS AT MAGNETIC DOMAIN WALLS

Interferometry of Majorana fermions requires the ability to transport Majorana fermions along two different paths and then recombining them.^{3,27,28,32,33} The semiconductor sandwich structure, in the appropriate parameter regime, contains propagating chiral Majorana fermion modes. However, as mentioned in the introduction, the Majorana fermions in these structures are neutral and therefore cannot be directly controlled by electrical voltages or measured as electrical currents. To avoid this difficulty, we will consider systems where a pair of isolated chiral Majorana modes propagating in the same direction are fused to form a chiral Dirac mode at a magnetic domain wall, which, as we will show, carries a measurable electrical current.

To model a domain-wall consisting of two isolated edges (marked 1 and 2 in Fig. 1) in the semiconductor, we will take $V_z(x) > 0$ ($V_z(x) < 0$) for $x < -\frac{W}{2}$ ($x > \frac{W}{2}$) and $V_z(x) = 0$ in between. Opposite V_z on the two sides of the edge can be realized by depositing separate magnetic insulators with opposite magnetization. As shown in Ref. [9], for $V_z = 0$ the system is a (non-topological) regular s -wave superconductor. Therefore, in the geometry in Fig. 1 there are two isolated edges in the semiconductor each separating contiguous domains of non-Abelian ($V_Z^2 > (\Delta^2 + \mu^2)$) and regular s -wave superconducting phases.

Since the Hamiltonian is translationally symmetric along the y -direction, we can factorize the energy eigenstates as $\psi_{k_y}(x, y) = e^{ik_y y} \phi_{k_y}(x)$ so that the solutions for $\phi_{k_y}(x)$ are determined by the y -independent Hamiltonian, obtained from Eq. (13) by the substitution $\partial_y \rightarrow ik_y$.

The second-quantized current operator in the spin-orbit

coupled semiconductor is given by⁴²,

$$\begin{aligned} \hat{J}(\mathbf{r}) = & \sum_{\beta} i \left[\nabla \hat{c}_{\beta}^{\dagger}(\mathbf{r}) \hat{c}_{\beta}(\mathbf{r}) - \hat{c}_{\beta}^{\dagger}(\mathbf{r}) \nabla \hat{c}_{\beta}(\mathbf{r}) \right] \\ & + \alpha \sum_{\beta, \gamma} \hat{c}_{\beta}^{\dagger}(\mathbf{r}) (\hat{z} \times \boldsymbol{\sigma})_{\beta\gamma} \hat{c}_{\gamma}(\mathbf{r}). \end{aligned} \quad (15)$$

The current carried by the quasi-particle $\hat{\gamma}^{\dagger}$ is then given by

$$\langle \hat{J} \rangle_{\gamma} \equiv \langle \Psi | \hat{\gamma} \hat{J} \hat{\gamma}^{\dagger} | \Psi \rangle - \langle \Psi | \hat{J} | \Psi \rangle, \quad (16)$$

where $|\Psi\rangle$ is the ground state. From the above equations, the expression for the quasiparticle current along y reduces to

$$\langle \hat{J}_y \rangle_{\gamma} = \int dx \phi_{k_y}^{\dagger}(x) (2k_y + \alpha \sigma_x) \phi_{k_y}(x). \quad (17)$$

In what follows, we will take the y -current operator in the BdG notation to be $J_y = (2k_y + \alpha \sigma_x)$.

The magnetic domain wall composed of magnetic layers of opposite magnetization (Fig. 1) is the key idea underlying our proposed Majorana interferometer since it enables an effective conversion of neutral Majorana modes into measurable charged current modes with current given by Eq. 17.

IV. CONDUCTANCE IN THE WIDE DOMAIN-WALL LIMIT

In the limit of $W \rightarrow \infty$, we can think of the interface as being composed of two isolated edges at $\pm W/2$. Zero-energy, $k_y = 0$, solution at each of these edges is particle-hole symmetric, *i.e.*, they satisfy $\phi_j(x) = \sigma_y \tau_y \phi_j^*(x)$ where j takes values 1 or 2, corresponding to 4-spinor wave functions at $-W/2$ ($\phi_1(x)$), and at $W/2$ ($\phi_2(x)$), respectively. The particle-hole transformation is defined as $\Xi = \sigma_y \tau_y K$ where K is the complex conjugation operator. Alternatively, the Majorana state ϕ_j can be written in a manifestly particle-hole symmetric form $\phi_j(x) = (u_j(x), -i\sigma_y u_j^*(x))^T$. The solution $u_1(x)$ is real and inside the interface falls off as

$$u_1(x) = u_1^*(x) = e^{-Re(z)x} [\rho e^{-Im(z)x} + c.c.] \quad (18)$$

where ρ is a constant 2-spinor and $z \approx (\frac{1}{\xi} + ik_F)$ with $\xi = \frac{v_F}{\Delta}$. Since $V_Z(x) = V_Z(-x)$, the Hamiltonian commutes with $\sigma_x P$ where P is the reflection operator with respect to the x axis. Hence, $\sigma_x P$ maps the Majorana mode $\phi_1(x)$ localized at $-W/2$ to the mode localized at $W/2$, *i.e.*, $\sigma_x P \phi_1(x) = \sigma_x \phi_1(-x) = \lambda \phi_2(x)$ where λ is a phase factor ($\lambda^* = \lambda^{-1}$). After some straightforward algebra, the requirement that both $\phi_1(x)$ and $\phi_2(x)$ are particle-hole symmetric requires $\lambda^2 = -1$ or $\lambda = i$. Using $k.p$ perturbation theory, the solutions $\phi_{j,k_y}(x)$ at $k_y \neq 0$ can be approximated to lowest order in k_y by $\phi_{j,k_y}(x) \approx \phi_j(x)$ and have energy $\epsilon_k = v_g k_y$ where

$$v_g = \alpha \langle \phi_j | \sigma_x \tau_z | \phi_j \rangle = 2 \int dx u_j^{\dagger}(x) \sigma_x u_j(x) \quad (19)$$

is the group velocity of the modes.

The BdG current operator (Eq. 17) for the Majorana states around $k_y = 0$ is given by $J_y = \alpha \sigma_x$. For $W \rightarrow \infty$, we get the current carried by the Majorana states ϕ_j to be

$$\begin{aligned} \langle \phi_j | J_y | \phi_j \rangle &= \alpha \int dx u_j^\dagger \sigma_x u_j + u_j^T \sigma_y \sigma_x \sigma_y u_j^* \\ &= \alpha \int dx u_j^\dagger \sigma_x u_j - u_j^\dagger \sigma_x u_j = 0, \end{aligned}$$

as expected.

For finite W , the wave functions ϕ_j are no longer orthogonal and have finite overlaps. Following Ref. [43], the lowest energy eigenstates for a finite-width interface can be considered to be superpositions of $\psi_{j,k_y}(x,y) = e^{ik_y y} \phi_j(x)$. Since $\sigma_x P$ commutes with the Hamiltonian, these eigenstates should be $\psi_{\pm,k_y}(x,y) = e^{ik_y y} \zeta_{\pm}(x)$ such that $\sigma_x P \zeta_{\pm}(x) = \pm \zeta_{\pm}(x)$. Using $\phi_2(x) = \lambda^{-1} \sigma_x \phi_1(-x)$ in the above it follows that

$$\zeta_{\pm}(x) = \frac{1}{\sqrt{2}} [\phi_1(x) \pm \iota \phi_2(x)]. \quad (20)$$

The expectation value of an operator A with respect to these energy eigenstates, to lowest order in the overlap, is given by

$$\begin{aligned} \langle \zeta_{\pm} | A | \zeta_{\pm} \rangle &= \frac{\sum_j \langle \phi_j | A | \phi_j \rangle \pm 2 \text{Im}(\langle \phi_1 | A | \phi_2 \rangle)}{2 \pm 2 \text{Im}(\langle \phi_1 | \phi_2 \rangle)} \\ &\approx \frac{1}{2} \sum_j \langle \phi_j | A | \phi_j \rangle \pm \text{Im}(\langle \phi_1 | A | \phi_2 \rangle). \quad (21) \end{aligned}$$

Using the above formula we can compute the excitation spectrum of a finite-width interface as

$$\epsilon_{\pm}(k_y) = \langle \zeta_{\pm} | H_{BdG}(k_y) | \zeta_{\pm} \rangle = v_g k_y \pm \alpha M \quad (22)$$

where M can be written as⁴⁴,

$$M = \partial_x \left[\phi_1^\dagger(x) \sigma_x \tau_z \phi_1(x) \right]_{x=0} = 2 \partial_x \left[u_1^\dagger(x) \sigma_x u_1(x) \right]_{x=0} \quad (23)$$

Thus, for finite W , tunneling splits the pair of chiral Majorana modes into a pair of modes with dispersion $\epsilon_{\pm}(k_y) = v_g(k_y \pm k_1)$ where $k_1 = \alpha M / v_g$.

The states ζ_{\pm} , unlike their constituent states ϕ_j , can carry a charge current. The expectation value of the current operator in these states is given by the cross-term

$$\begin{aligned} \alpha \langle \phi_1 | \sigma_x | \phi_2 \rangle &= \alpha \int dx u_1^\dagger \sigma_x u_2 + u_1^T \sigma_y \sigma_x \sigma_y u_2^* \\ &= 2i\alpha \int dx \text{Re}(u_1^\dagger(x) u_1(-x)), \quad (24) \end{aligned}$$

which is now non-zero as advertised in the introduction. Let us now estimate the conductance of the interface using the states ζ_{\pm} ⁴⁵. The branches $\psi_{\pm,k_y}(x,y)$ are related by particle-hole conjugation. Therefore it suffices to consider the occupancy of only the electron-like branch defined by $\langle \tau_z \rangle > 0$. Only the sign of the current $\langle \hat{J}_y \rangle$ depends on which of the two particle-hole conjugate branches is electron-like. Therefore, we assume the $+$ branch to be electron-like and multiply the

result by the sign of $\langle \tau_z \rangle_+ = 2 \int dx u_1^T(-x) \sigma_x u_1(x)$ at the end of the calculation. For a finite bias voltage V , which is applied to the interface by coupling it to a reservoir at a chemical potential ($\mu_S + eV$) via a tunnel barrier, the occupation function of the mode is given by $f(\epsilon_+(k_y) - eV)$ where $f(\epsilon)$ is the Fermi function⁴⁵. The conductance of the interface for $V \rightarrow 0$ can be computed using a Landauer-like formula

$$G(0) = \frac{d}{dV} \int dk_y f(\epsilon_+(k_y) - eV) \langle \hat{J}_y \rangle_{+,k_y} |_{V=0} = \frac{\langle \hat{J}_y \rangle_{+,-k_1}}{v_g} G_0 \quad (25)$$

where G_0 is the quantum of conductance. Substituting the explicit form for the expectation value with respect to the energy eigen-modes (Eq. 21), $G(0)$ can be written as

$$G(0) = \frac{2G_0}{v_g} \text{sgn}(\langle \tau_z \rangle_+) \left[-k_1 + \int dx \text{Re}(u_1^\dagger(x) u_1(-x)) \right]. \quad (26)$$

Using the asymptotic form of the chiral edge state wavefunctions (Eq. (18)), the above expression, in the large W limit, can be shown to be of the form

$$G(0) \sim \text{sgn}(\langle \tau_z \rangle_+) e^{-\text{Re}(z)W} \cos(2\text{Im}(z)W + \delta) G_0 \quad (27)$$

where δ is a phase-shift. As claimed in the introduction, this is finite for finite interface width, but vanishes exponentially with W with a decay length $\text{Re}(z)^{-1} = \xi$.

V. NUMERICAL SOLUTION FOR NARROW DOMAIN-WALLS

For experimental purposes, it is interesting to consider the limit where the width of the interface W is much smaller than the coherence length ($W \ll \xi$) of the superconductor. For definiteness we approximate this limit as $W = 0$, in which case there is a single interface at $x = 0$.

As in the wide-interface case, the zero-bias conductance can be written in terms of the $E = 0$ energy eigenstate $\psi_{+,-k_1}(x,y) = e^{-ik_1 y} \zeta_+(x)$, which is determined by its value on one side of the interface, say $x > 0$, where it can be expanded as $\zeta_+(x) = \sum_{n: \text{Re}(z_n) < 0} c_n e^{z_n x} \phi_n$. Here ϕ_n and z_n are complex eigenvectors and eigenvalues of the Hamiltonian $H_{BdG}(k_y, z)$ in Eq. [13] (with the substitutions $\partial_x \rightarrow z$ and $\partial_y \rightarrow ik_y$), *i.e.*, they satisfy $H_{BdG}(k_y, z_n) \phi_n = 0$. The boundary conditions at $x = 0$ are then given by $\sigma_x \zeta_+(0) = \zeta_+(0)$ and $\sigma_x \zeta_+'(0) = -\zeta_+'(0)$. We vary k_y on the real axis to find the value $k_y = -k_1$ where the boundary conditions on the wave function are satisfied. The expectation value of an observable A is calculated as

$$\langle A \rangle = \int dx \zeta_+^\dagger(x) A \zeta_+(x) = \sum_{n,m} c_n^* c_m \frac{\phi_n^\dagger(A + \sigma_x A \sigma_x) \phi_m}{z_m + z_n^*}. \quad (28)$$

We numerically calculate c_n for a representative set of parameter values appropriate for the non-Abelian superconducting phase: $\Delta = 0.5$, $\mu = 0.2$, $\alpha = 1.0$ in units where all energies are scaled by $V_Z = 1$ meV and lengths are scaled by

$\hbar/\sqrt{2m^*V_Z^9}$. In this calculation, the conductance in the limit $V \rightarrow 0$ is found to be $G(0) = 0.88G_0$. To avoid decoherence processes such as scattering of electrons into holes, we find that $V, T < k_1 v_g \sim 0.1$ meV where T is the temperature.

VI. DOMAIN-WALL BASED MAJORANA FERMION INTERFEROMETERS

Since the interface between two domains of the semiconductor heterostructure with opposite directions of Zeeman splitting carries a charge current, constructing electrically controlled Majorana interferometry experiments^{32,33} is straightforward. In Fig. 2a, the interfaces a and d carry charge current. In contrast to interfaces a and d , the edges b and c separate a non-Abelian superconducting phase from the vacuum in the central hole. Hence, they carry charge-neutral Majorana modes which we denote by γ_{0b}, γ_{0c} . At the tri-junction between the edges a, b , and c , a chiral charged quasiparticle or quasihole in interface a breaks into a pair of Majorana fermions in b and c : $c_a^\dagger \rightarrow \gamma_{0b} + i\gamma_{0c}$, $c_a \rightarrow \gamma_{0b} - i\gamma_{0c}$. There are an even (including zero) or odd number n_V of flux quanta threaded into the central hole in the interferometer. Consequently, for an odd (even) number of vortices in the central hole, only one (none) of γ_{0b} and γ_{0c} encounters a change of sign while traversing the edges b and c . It follows that, for an odd number of vortices in the central hole, $c_a^\dagger \rightarrow c_d$ and $c_a \rightarrow c_d^\dagger$ (a quasiparticle incident from a turns into a quasihole at d or vice versa), and charge $2e$ is transferred between the interface a and the superconductor. Therefore, if the number of vortices in the hole is odd (even), there is a non-zero (zero) current between the interface a and the superconductor, which is a definitive signature of non-Abelian statistics of the Majorana quasiparticles.

We now consider an interferometer geometry capable of measuring the fermion number in a topological qubit made of two vortices (Fig 2b). Such a measurement is important for TQC in the semiconductor.²⁹⁻³¹ Charged fermion quasiparticles carrying current I at the left interface break up into two Majorana fermions at edges b and d . The Majorana fermion at d can quantum mechanically tunnel to edge c via two edge constrictions on the two sides of the central qubit. We assume that the constrictions have small enough capacitance so that the Majorana fermion tunneling amplitudes t_1, t_2 via *vortex tunneling* (quantum phase slips) are appreciable in the background of superconducting quasiparticle tunneling. Writing the net such tunneling amplitude as t_{dc} and the number of fermions trapped in the central qubit as n_f , we get⁴⁶,

$$t_{dc} \propto t_1^2 + t_2^2 + (-1)^{n_f} 2t_1 t_2. \quad (29)$$

Here, the factor of $(-1)^{n_f}$ arises from the phase picked up by a vortex on one full circle around n_f fermions. It follows that for $t_1 \sim t_2$ the contribution to the current from quantum phase slips at the two constrictions vanishes for an odd number of fermions at the center. Therefore, with change in n_f at the central qubit, the magnitude of the current I shows well defined oscillations. We note that quantum vortex tunneling,

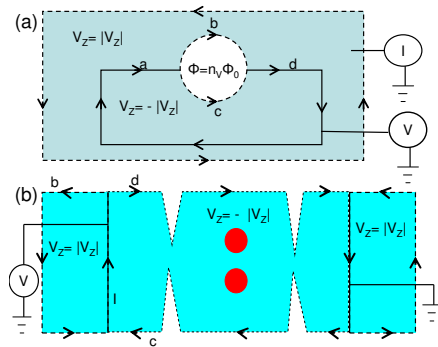


FIG. 2: (a): Interferometer geometry to test non-Abelian statistics of Majorana fermions. There is a non-zero current I flowing in the superconductor when the number of vortices n_V in the central hole is odd. ϕ_0 indicates the superconducting flux quantum $\frac{hc}{2e}$; (b): Interferometric measurement of the fermion number in a pair of vortices shown as (red) circles forming a qubit at the center. Charged fermion quasiparticles carrying current I break into Majorana modes along edges b and d , which can recombine after quantum tunneling at the two edge constrictions on the two sides of the qubit.

i.e. quantum phase slip, is an essential ingredient of our interferometer.

VII. CONCLUSION

The electrically controlled edge-state interferometry on the semiconductor heterostructure we propose in this paper are exactly analogous to those proposed previously for the non-Abelian states in the $\nu = 5/2$ fractional quantum Hall system and on the surface of a 3D strong topological insulator.^{3,27,28,32,33} The Majorana fermion edge excitations on the fractional quantum Hall systems are charged^{3,27,28} and charged edge modes have also been shown to be possible on the surface of a 3D topological insulator.^{32,33} Even though the charge of the edge excitations make electrically controlled interferometry fairly straightforward in these systems, there have been lingering questions if such experiments are possible on the semiconductor structure because of the absence of charge of the chiral modes on any isolated edge in this system. In this paper we have shown that two isolated edges carrying individually charge-less Majorana edge modes can be *superposed* to create an edge which does carry charge. The charge of this new edge mode can be used to electrically control edge currents which in turn can be used in the interferometry experiments. Quantum phase slips, which are essential for our scheme to work have been experimentally observed,⁴⁷ and therefore, our scheme should work as a matter of principle.

There is a natural sequence of experiments in the study of Majorana modes in the semiconductor sandwich structures. The first experiments, which are already underway,⁴⁸ would fabricate the appropriate SC/Sm heterostructures searching for the proximity-induced superconductivity in the appropriate parameter space of chemical potential and Zeeman splitting. Once superconductivity is identified in the semicon-

ductor, suitable tunneling spectroscopic measurements would have to establish a robust zero-energy anomaly in the semiconductor consistent with the existence of the zero-energy Majorana mode. One great advantage of the sandwich structure is the generic existence of the Majorana mode by construction in the topological superconducting phase in contrast to the $5/2$ FQHE state where the non-Abelian ground state is a conjecture. The observation of the zero-bias anomaly showing the existence of a zero-energy state in the BdG spectrum would satisfy the necessary condition for the existence of the Majorana mode, but not the sufficient condition. The proposed fractional Josephson effect experiment^{14,41} would provide the sufficient condition, but direct interferometry, as proposed in the current work, is essential in establishing the non-Abelian nature of the Majorana particles. What we propose here is not by any means an easy experiment, but it is probably not much harder than the on-going interferometric measurements⁴⁹ in the $5/2$ FQHE state. We emphasize that only interferometry can directly establish the existence of non-Abelian braiding statistics, and as such our proposed

experiment is an important necessary step in the beautiful and exotic physics of emergent solid state non-Abelian modes.

Our proposed interferometry experiments give clear cut signatures of the non-Abelian statistics of the Majorana modes localized in the order parameter defects on the semiconductor heterostructure. In addition to the zero-bias conductance peak experiments¹¹ and the experiments measuring the fractional Josephson effect^{14,17} due to Majorana fermions, these experiments constitute another class of measurements directly testing the existence of non-Abelian quasiparticles in the semiconductor heterostructure. Moreover, the interferometry experiments, like their counterparts in the $\nu = 5/2$ state and on the surface of a topological insulator, constitute the necessary first step in entanglement generation and implementation of TQC using the 2D semiconductor heterostructure.

We thank Roman Lutchyn for discussions. This work is supported by DARPA-QuEST, JQI-NSF-PFC, and LPS-NSA. ST acknowledges DOE/EPSCoR Grant # DE-FG02-04ER-46139 and Clemson University start up funds for support.

-
- ¹ A. Kitaev, *Annals Phys.* **303**, 2 (2003).
² C. Nayak, S. H. Simon, A. Stern, M. Freedman, and S. Das Sarma, *Rev. Mod. Phys.* **80**, 1083 (2008).
³ S. Das Sarma, M. Freedman, and C. Nayak, *Phys. Rev. Lett.* **94**, 166802 (2005).
⁴ N. Read and D. Green, *Phys. Rev. B* **61**, 10267 (2000).
⁵ D. A. Ivanov, *Phys. Rev. Lett.* **86**, 268 (2001).
⁶ S. Das Sarma, C. Nayak, and S. Tewari, *Phys. Rev. B* **73**, 220502 (R) (2006).
⁷ S. Tewari, S. D. Sarma, C. Nayak, C. Zhang, and P. Zoller, *Phys. Rev. Lett.* **98**, 010506 (2007).
⁸ L. Fu and C. L. Kane, *Phys. Rev. Lett.* **100**, 096407 (2008).
⁹ Jay D. Sau, R. M. Lutchyn, S. Tewari, S. Das Sarma, *Phys. Rev. Lett.* **104**, 040502 (2010).
¹⁰ S. Tewari, Jay D. Sau, S. Das Sarma, *Annals Phys.* **325**, 219-231 (2010).
¹¹ J. D. Sau, S. Tewari, R. Lutchyn, T. Stanescu and S. Das Sarma, *Phys. Rev. B* **82**, 214509 (2010).
¹² J. Alicea, *Phys. Rev. B* **81**, 125318 (2010).
¹³ M. Franz, *Physics*, 3,24 (2010).
¹⁴ R. M. Lutchyn, Jay D. Sau, S. Das Sarma, *Phys. Rev. Lett.* **105**, 077001 (2010).
¹⁵ P. Bonderson, S. Das Sarma, M. Freedman, C. Nayak, arXiv:1003.2856.
¹⁶ X. Qi, T. Hughes, S. Zhang, *Phys. Rev. B* **82**, 184516 (2010).
¹⁷ Y. Oreg, G. Refael, F. V. Oppen, *Phys. Rev. Lett.* **105**, 177002 (2010).
¹⁸ D. Linder, A. Sudbo, *Phys. Rev. B* **82**, 085314 (2010).
¹⁹ Tewari, S., Stanescu, T. D., Sau, J. D., Das Sarma, S., *New J. Phys.* **13**, 065004 (2011).
²⁰ Hassler, F., Akhmerov, A. R., Hou, C.-Y., Beenakker, C. W. J. *New J. Phys.* **12**, 125002 (2010).
²¹ Sau, J. D., Tewari, S., Das Sarma, S., *Phys. Rev. A* **82**, 052322 (2010).
²² R. M. Lutchyn, Tudor Stanescu, S. Das Sarma, *Phys. Rev. Lett.* **106**, 127001, 2011.
²³ T. Stanescu, R. M. Lutchyn, S. Das Sarma arXiv:1106.3078 (2011).
²⁴ I. Serban, B. Beri, A. R. Akhmerov, and C. W. J. Beenakker, *Phys. Rev. Lett.* **104**, 147001 (2010).
²⁵ L. Mao, M. Gong, E. Dumitrescu, S. Tewari, C. W. Zhang, arXiv:1105.3483
²⁶ S. Tewari, J. D. Sau, V. W. Scarola, C. Zhang, S. Das Sarma, arXiv: 1106.5506
²⁷ A. Stern and B. I. Halperin, *Phys. Rev. Lett.* **96**, 016802 (2006).
²⁸ P. Bonderson, A. Kitaev, and K. Shtengel, *Phys. Rev. Lett.* **96**, 016803 (2006).
²⁹ S. Bravyi, A. Kitaev *Phys. Rev. A* **71**, 022316 (2005).
³⁰ S. Bravyi, *Phys. Rev. A* **73**, 042313 (2006).
³¹ P. Bonderson, M. Freedman, and C. Nayak, *Ann. Phys. (New York)* **324**, 787 (2008).
³² L. Fu and C. L. Kane, *Phys. Rev. Lett.* **102**, 216403 (2009).
³³ A. R. Akhmerov, J. Nilsson, and C. W. J. Beenakker, *Phys. Rev. Lett.* **102**, 216404 (2009).
³⁴ E. Grosfeld, B. Seradjeh, S. Vishveshwara, *Phys. Rev. B* **83**, 104513 (2011).
³⁵ E. Grosfeld, A. Stern, arXiv:1012.2492 (2011).
³⁶ A. Chrestin, T. Matsuyama, and U. Merkt, *Phys. Rev. B* **55**, 8457 (1997).
³⁷ J. Nogués and I. Schuller, *J. Magn. Magn. Mat.*, **192**, 203 (1999).
³⁸ T. Stanescu, J. D. Sau, R. Lutchyn and S. Das Sarma, *Phys. Rev. B* **81**, 241310R (2010).
³⁹ P. G. de Gennes, *Rev. Mod. Phys.* **36**, 225 (1964).
⁴⁰ J. D. Sau, R. M. Lutchyn, S. Tewari, and S. Das Sarma, *Phys. Rev. B* **82**, 094522 (2010).
⁴¹ A. Y. Kitaev, *Physics-Uspekhi* **44**, 131 (2001).
⁴² A. A. Burkov, Alvaro S. Núñez, and A. H. MacDonald, *Phys. Rev. B* **70**, 155308 (2004).
⁴³ M. Cheng, R. M. Lutchyn, V. Galitski, and S. Das Sarma, *Phys. Rev. Lett.* **103**, 107001 (2009).
⁴⁴ J. Bardeen, *Phys. Rev. Lett.* **6**, 57 (1961).
⁴⁵ G. E. Blonder, M. L. Tinkham and T. M. Kalpwijk, *Phys. Rev. B* **25**, 4515 (1982).
⁴⁶ E. Fradkin, C. Nayak, A. M. Tsvelik, and F. Wilcek, *Nucl. Phys. B* **516**, 704 (1998).
⁴⁷ V. E. Manucharyan, N. A. Masluk, A. Kamal, J. Koch, L. I.

- Glazman, M. H. Devoret, arXiv:1012.1928 (2010).
- ⁴⁸ Kouwenhoven, private communications; Marcus, private communications; Martinis, private communications; Gervais, private communications.
- ⁴⁹ R. L. Willett, L. N. Pfeiffer, K. W. West, Phys. Rev. B **82**, 205301 (2010); R.L. Willett, L.N. Pfeiffer, K.W. West, arXiv:0911.0345.